



**ARTICLE**

## Effect of Alkaline Electrolyzed Water on Performance Improvement of Green Concrete with High Volume of Mineral Admixtures

Guibin Liu<sup>1</sup>, Meinan Wang<sup>2</sup>, Qi Yu<sup>1</sup>, Qiuyi Li<sup>2</sup> and Liang Wang<sup>2,\*</sup>

<sup>1</sup>Center for Technological Development, Qingdao Qingjian New Material Group Co., Ltd., Qingdao, 266108, China

<sup>2</sup>College of Civil Engineering & Architecture, Qingdao Agricultural University, Qingdao, 266109, China

\*Corresponding Author: Liang Wang. Email: Liangwang2019@qau.edu.cn

Received: 16 December 2020 Accepted: 20 February 2021

### ABSTRACT

The strength and durability of concrete will be significantly reduced at high volume of mineral admixture, and the poor early strength of concrete also still needs to be solved. In this investigation, a highly active alkaline electrolyzed waters was used as mixing water to improve the early strength and enhance the durability of green concrete with high volume mineral admixture, the influences of alkaline electrolyzed water (AEW) on hydration activity of mineral admixture and durability of concrete were determined. The results showed that compared with natural tap water, AEW can accelerate early hydration process of cement in concrete and produce comparatively more hydrated products, leading to a 13.6% higher compressive strength than that of ordinary concrete at early age, but the improvement effect of AEW concrete was relatively reduced at long-term age. Meanwhile, the activity of mineral admixtures could be stimulated by AEW to some extent, the strength and durability performance of AEW concrete after double doping 25% slag and 25% fly ash can still reach the level of ordinary cement concrete without mineral admixtures. The SEM micromorphology of 7 d hydrated natural tap water cement paste was observed to be flaky and tabular, but the AEW cement pastes present obvious cluster and granulation phenomenon. The SEM microstructure of AEW concrete with mineral admixtures is more developed and denser than ordinary tap water concrete with mineral admixtures. Therefore, the AEW probably could realize the effective utilization of about 50% mineral admixture amount of concrete without strength loss, the cement production cost and associated CO<sub>2</sub> emission reduced, which has a good economic and environmental benefit.

### KEYWORDS

Alkaline electrolyzed water; durability improvement; green concrete; mineral admixture; micromorphology

## 1 Introduction

The attendant massive pile of industrial waste not only polluted environment but also caused the waste of resources with the global process of industrialization, the large amount of industrial waste residue is used for concrete as mineral admixture, which can fully meet the requirements of the sustainable development of human society [1]. At present, high performance green concrete has been widely used in modern concrete structures, which is characterized by the use of mineral admixtures, such as fly ash and ground granulated blast furnace slag [2–5]. Considering that using mineral admixtures to replace part of cement can substantially decrease the hydration temperature rise of concrete and reduce the cracking risk of concrete



[6,7], maximizing the use of mineral admixture under the premise of ensuring the high performance of concrete can promote the mechanical properties and durability of concrete and achieve the purpose of reducing cement, saving resources, green and environment friendly [8]. However, a large amount of researches showed the small percentage of singly-doped mineral admixture is beneficial in optimizing the workability and low cost but it may not improve the durability to any considerable extent [9–12], and the strength and durability of concrete will be significantly reduced at high volume [13–15], Faiz et al. [16] reported the reduction of 28 d compressive strength of concrete was 15.82%, 19.34% and 48.99% with the increase of 50%, 60% and 70% fly ash, respectively. By comparison, although multi-doped mineral admixtures can increase the replacement ratio to a certain extent, improve concrete workability and pumpability [17], the strength and durability of concrete with high volume mineral admixture is worse than that of ordinary concrete [18–20]. More important is that low early activity of mineral admixture and poor early strength of concrete still need to be solved [21].

The alkaline electrolyzed water (AEW) is a kind of highly active water, which has been widely used in food hygiene, environmental cleaning, agricultural industries, etc. [22–24]. Sun et al. [25] researched that mixing alkaline water can decrease the total porosity of concrete and increase the strength by 21%. Kimura et al. [26] showed that electrolyzed water can decrease the amount of maximum radiation ray rate by up to 10% than ordinary water mortar. Mandal et al. [27] indicated that electrolyzed water can reduce the initial and final setting time of cement. Chakraborty et al. [28] revealed the electrolyzed water in can enhance the mechanical properties of cement mortar at the fresh and early hardened states. In this investigation, a kind of AEW was used in green concrete with high volume mineral admixture as mixing water, which is expected to be beneficial not only for promoting the early hydration of cement, improving the early and late strength, enhancing the durability of concrete, but also it can be considered as a greener admixture for minimizing the cement consumption and construction cost, which can provide a new way and reference for the engineering application of concrete with high volume of mineral admixtures.

## 2 Experimental Programs

### 2.1 Experimental Materials

The ordinary Portland cement (P·O 42.5) was provided by Shanlv Cement Co., Ltd. (Qingdao, China) in this study, which met the requirements of “PRC standards for Portland cement and ordinary Portland cement”(GB 175-2007). The density is 3.16 g/cm<sup>3</sup>, the surface area is 3350 cm<sup>2</sup>/g, the fineness is 2.3%. The S95 grade granulated blast furnace slag (GGBFS) was used in this study, the specific surface area >400 m<sup>2</sup>/kg, the density is 2.88 g/cm<sup>3</sup>, loss on ignition is less than 1.0%, meeting the requirements of “Ground granulated blast furnace slag for cement, mortar and concrete” (GB/T18046-2017). The I-class fly ash was provided by Weifang Huadian Co., Ltd., Weifang, China, the density is 2.24 g/cm<sup>3</sup>, water requirement ratio is 0.95, loss on ignition is 1.1%, which meets the requirements of “Fly ash used for cement and concrete” (GB/T 1596-2017), the XRF results of different mineral admixtures are shown in Tab. 1. The natural river sand was used as fine aggregate, crushed quartzite stone were used as coarse aggregate with 5–31.5 mm continuous grading. The detailed parameters of fine and coarse aggregates are shown in Tabs. 2 and 3, respectively. The NC-J type polycarboxylate superplasticizer was used, which is produced by Shandong Academy of Building Science, the water-reducing ratio was 28% at 2.0–2.2% dosage of the cement weight, the ratio of bleeding rate is less than 30%, and the content of chloride ion is not more than 0.06%.

**Table 1:** Chemical composition results of different mineral admixtures by XRF (%)

Type	CaO	SO <sub>3</sub>	SiO <sub>2</sub>	Al <sub>2</sub> O <sub>3</sub>	MgO	Fe <sub>2</sub> O <sub>3</sub>	CO <sub>2</sub>	TiO <sub>2</sub>	Others
Portland Cement	52.71	2.60	19.9	6.41	4.60	2.83	9.50	0.40	1.05
I-class Fly ash	8.20	1.40	48.8	25.2	1.30	6.50	3.90	1.60	3.10
Blast furnace slag	36.40	2.00	29.1	14.3	8.90	0.30	5.60	1.30	2.10

**Table 2:** Performance index of natural fine aggregate in this study

Fineness module	Specifications	Stacking density/( $\text{kg}\cdot\text{m}^3$ )	Apparent density/( $\text{kg}\cdot\text{m}^3$ )	Void ratio/%	Micro powder content/%	Mud content/%	Crushing index/%
2.40	II class sand	1450	2590	40	1.00	0.70	13.1

**Table 3:** Performance index of natural coarse aggregate in this study

Water absorption/%	Moisture content/%	Content of needle-like particles/%	Crushing index/%	Stacking density / ( $\text{kg}\cdot\text{m}^3$ )	Apparent density /( $\text{kg}\cdot\text{m}^3$ )
1.70	0.42	4.05	11.2	1460	2510

## 2.2 Production and Preparation of AEW

A kind of highly active AEW was used as mixing water to prepare concrete with high volume of mineral admixtures in this study. The AEW was prepared by Boxin BX-SQJ series fully automatic ion-exchange diaphragm alkaline electrolytic water equipment, as shown in Fig. 1. Pure water was electrolyzed to avoid the influence of impurities in water on experimental results, potassium carbonate (AR) was used as electrolyte, the concentration of  $\text{K}_2\text{CO}_3$  electrolyte is 0.05%, the voltage of electrolysis is 380 V 50 Hz, the water inlet temperature: 10–30°C, the total inlet water flow was 32.5 L/H, the inlet alkaline water flow was 20 L/H, the electrolysis's time was 15 min, the pH of AEW was about 9.8 at this time. By adjusting the current, voltage, influent flow and electrolysis time, the AEW with different performance can be prepared. Under the condition of constant voltage, the concentration of  $\text{K}_2\text{CO}_3$  electrolyte and current value should be increased when pH value increased.

**Figure 1:** Diaphragm type electrolytic cell

In an electrolyzing cell with diaphragm, due to  $\text{K}_2\text{CO}_3$  electrolyte solution of definite concentration of electrolytic treatment, KOH is generated on the cathode, the water is decomposed into hydrogen and hydroxyl ions; meanwhile, carbonic acid is generated on the anode, the  $\text{H}_2\text{O}$  is decomposed into oxygen and hydrogen ions, it is an acid solution [29]. The schematic diagram of electrolysis principle is shown in Fig. 2. Ordinary tap water was used as mixing water for blank comparative analysis, the pH meter and ORP meter are shown in Figs. 3 and 4, which were used to test the pH and ORP values of AEW in this

study, ORP is the abbreviation of redox potential, which represents the relative oxidation or reduction degree of AEW [30], the detailed performance index of AEW is shown in Tab. 4.

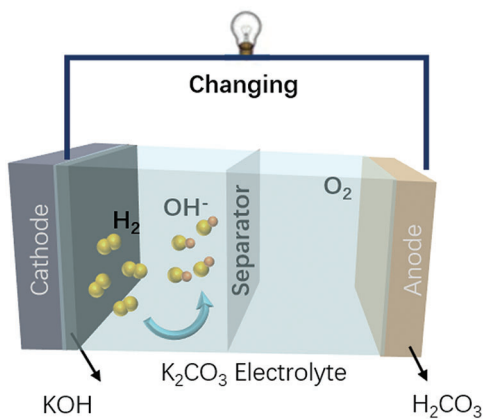


**Figure 2:** Schematic diagram of electrolysis



**Figure 3:** pH meter for electrolyzed water



**Figure 4:** ORP meter for electrolyzed water

**Table 4:** Performance index of different mixing water in this study

Type	Ideal pH range	pH measured value	ORP measured value	Abbreviations
Ordinary tap water	7	7.51	343	PT
K <sub>2</sub> CO <sub>3</sub> alkaline electrolyzed water	9~10	9.82	191	DJ

### 2.3 Mix Proportions Design

Tab. 5 presented the detailed mix proportions of different concrete with mineral admixture in this study. The cement content is 420 kg/m<sup>3</sup>, the actual water consumption is determined by controlling the slump of concrete mixture in the range of 180–220 mm, the sand coarse aggregate ratio (s/a) was designed as 50%. The proportion of total mineral admixtures to the total cementitious materials amount in concrete is designed as 0%, 40% and 50%, respectively, and the proportion of fly ash (FA) and blast furnace slag (BFS) is 1:1 by mass. The ordinary tap water concrete is blank control group, and the marks are A1, A2 and A3 in turn, the corresponding marks of AEW concrete are B1, B2 and B3, respectively. The dosage of water reducer admixture to the cement amount was 2.0%–2.2%, the water reducing ratio is 28%–30%.

**Table 5:** Mix proportion design of different concrete with high volume of mineral admixture

Type	Mark	C	BFS	FA	S	G	W	Ad
Natural tap water	A1	420	0	0	912	877	177	8.4
	A2	255	85	85	917	881	159	12.7
	A3	215	108	108	918	882	149	15.0
Alkaline electrolyzed water	B1	420	0	0	912	877	177	8.4
	B2	255	85	85	917	881	159	12.7
	B3	215	108	108	918	882	149	15.0

Note: C: cement; S: sand; G: stone; W: water; Ad: water-reducer admixture.

### 2.4 Experimental Methods

AEW and ordinary tap water were used to prepare different concretes with high volume of mineral admixtures. The slump of different concrete mixture was controlled in the range of 180–220 mm. According to “Standard for test method of mechanical properties of ordinary concrete” (GB/T 50081-2002) in China, three identical cubic concrete specimens were made into 150 mm × 150 mm × 150 mm for each specimen design. After demoulding, the concrete specimens are moved to the standard curing laboratory with the temperature of (20 ± 2)°C and the relative humidity of (90 ± 5)%, the compressive strength tests of specimens are carried out at different age of 3, 7, 14, and 28 d, respectively. Moreover, according to “Standard for test methods of long-term performance and durability of ordinary concrete” (GB/T 50082-2009), the chloride ion permeability test for concrete was conducted through the RCM method [31], the penetration coefficient of Cl<sup>-</sup> in concrete can be calculated out. The carbon dioxide concentration in the carbonization chamber was adjusted to (20 ± 3)%, the humidity was controlled at (70 ± 3)% and the temperature was controlled at (20 ± 2)%. The carbonation depth tests for different concretes were conducted to 3, 7, 14, 28 and 91 d [32]. Considering the factors such as test period and test conditions, the quick freezing method is used in the freeze-thaw cycle test of concrete. The concrete specimens were cured in the standard curing room until the age of 28 d, the mass loss of the test specimens was measured once every 25 freeze-thaw cycles, and the transverse fundamental frequency

was measured by dynamic modulus tester. The accuracy of relative dynamic modulus and mass loss rate in the test results are determined to be 0.1%. The X-ray diffraction analysis test was performed to characterize the mineral composition of cement paste in concrete at 7 d by XRD device (D8 Advance, Bruker AXS, Germany), the micromorphology of the different concrete was observed by scanning electron microscopy (SEM), and the microstructure of different concrete with high volume mineral admixture can be characterized by XRD and SEM spectra, the influence mechanism of AEW on the performance of high volume concrete can be analyzed eventually.

### 3 Results and Discussions

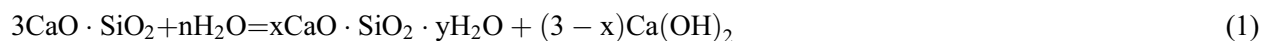
#### 3.1 Workability of Different Series of Concrete

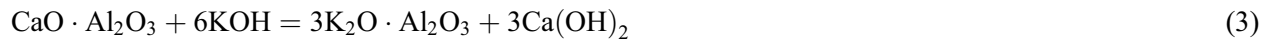
The slump testing of concrete was given in Fig. 5, from Fig. 6, it can be seen that the under the condition of the same slump range (180–220 mm), the water consumption of AEW concrete are all lower than those of natural tap water concrete at same proportioning. For ordinary cement concrete without mineral admixture, the water consumption of B1 AEW concrete reduced by 5 kg/m<sup>3</sup>. This is likely that AEW can accelerate hydration process and setting of cement, which is mainly governed by early dissolution of cement grains and rapid flocculation of hydrated products in presence of OH ions [33], as shown in Eqs. (1) and (2). Meanwhile, the highly active AEW small molecular group with negative charge could be absorbed on the surface of cement particles, which can make cement particles with same charge evenly disperse due to electrostatic repulsion and release more combined water in concrete [34], leading to a workability improvement of AEW concrete than that of natural tap water concrete. Behnam et al. [35–37] showed that using magnetized water instead of tap water leads to a higher slump flow and a lower viscosity of concrete due to high activity and small water molecular group after magnetization, which is similar to functional mechanism of AEW in concrete.



Figure 5: Slump testing of concrete

At the same time, at the early age, KOH in electrolyzed water was likely to react with the unhydrated  $\text{CaO} \cdot \text{Al}_2\text{O}_3$  in cement to produce potassium aluminate (a kind of condensation promoter), as shown in Eq. (3), which could promote the hydration rate and setting of cement, having a positive effect in improving the workability of concrete.





In addition, the water consumption of natural tap water and AEW concrete both decreased with the increase of mineral admixture content, which is mainly affected by the content of water reducer admixture.

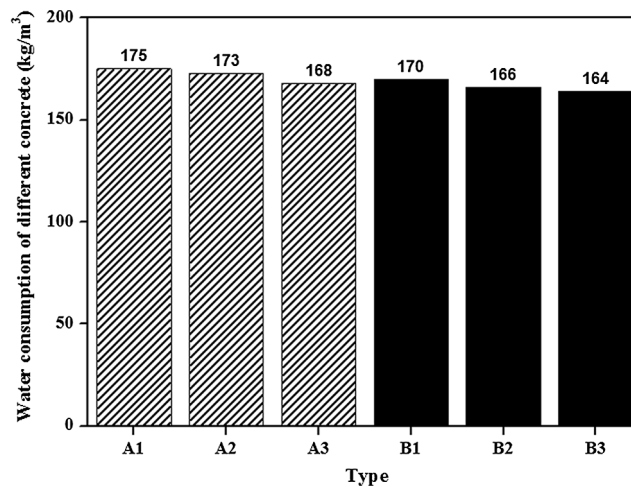


**Figure 6:** Water consumption of different concrete

### 3.2 Compressive Strength Development of Different Series of Concrete

From Fig. 7, it can be seen that the strength development of three AEW concretes at each curing age were all higher than those of natural tap water concrete at same proportioning, of which the strength improvement effect of B1 concrete was the best. Meanwhile, the strengths of natural tap water and AEW concrete both decreased with increasing mineral admixture content at each age. At the early age (3 d), the strengths of B1 and B2 AEW concrete increased by about 13.6% and 7.3% than that of A1 natural tap water concrete, and the strength of B3 concrete was slightly higher than that of A1 concrete. Sumit et al. [28] indicated a 16% higher compressive strength of electrolyzed water mortar than that of normal mortar at 3 d, Wang et al. [38] also showed a 20% strength improvement of electrolyzed water mortar, which is essentially in agreement with results in this study.

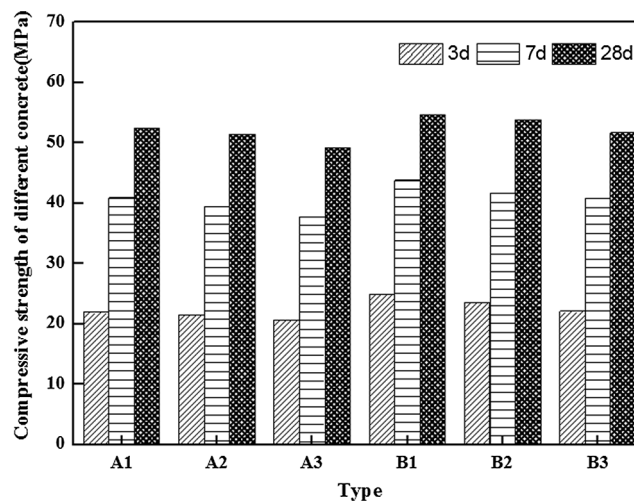


**Figure 7:** Compressive strength development of different series of concrete with curing age

In contrast, the strength growth rate of B1 and B2 AEW concrete at 28 d decreased significantly, increased by only 4.2% and 2.5% than that of A1 concrete, the strength of B3 concrete was close to that of A1 concrete, but the strengths of these three AEW concretes were obviously higher than those of A2 and A3 concrete. It showed that introducing the AEW in concrete can accelerate cement hydration and activate the activity of mineral admixtures, leading to an increase of strength at early age. However, at the long-term age, the cement hydration was also relatively sufficient, the activity and electrostatic repulsion of AEW decreased, the strength improvement effect of AEW concrete reduced.

### 3.3 Free-Thaw Cycles of Different Series of Concrete

From Fig. 8 and Fig. 9, the results showed that after 300 times freeze-thaw cycles, the relative dynamic elastic modulus loss and the weight loss rates of ordinary tap water concrete series was more evident than those of AEW concrete series. With the freeze-thaw cycles number increase, the declining rate of weight loss and relative loss modulus of AEW concrete series were slowed obviously, showing a better frost resistance, which can well meet the actual engineering requirements. Meanwhile, with the increasing of mineral admixture content in concrete, the freeze and thaw resistance of ordinary tap water concrete and AEW concrete are both reduced. Moreover, the freeze and thaw resistance of B3 AEW concrete can still reach the level of A1 ordinary concrete after double doping 25% slag and 25% fly ash, the relative dynamic elasticity modulus and weight loss ratio were 91.4% and 1.6%, which was superior to those of A2 and A3 ordinary tap water concrete.

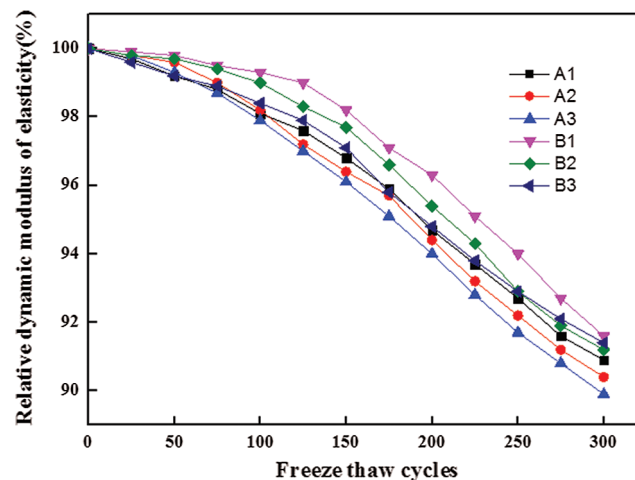


Figure 8: Relative dynamic elasticity modulus of concrete

### 3.4 Chloride Ion Penetration Property of Different Series of Concrete

The testing device for chloride permeability of different concrete is shown in Fig. 10, NJ-RCM Chloride diffusion coefficient tester for concrete, Beijing Naijiu Technology Co., Ltd., China, after standard curing, the cylinder concrete specimens were submerged in an ultrasonic bath for 15 min, then the positive and negative electrodes of specimens were immersed in the 0.2 mol/L KOH solution and 0.2 mol/L KOH solution containing 5%NaCl, respectively. The electric time was determined according to the initial electric current. The penetration coefficient of chloride ions of concrete was calculated by the penetration depth of chloride ions. The  $\text{Cl}^-$  penetration coefficients of ordinary tap water concrete and AEW concrete at different curing age are given in Fig. 11. From Fig. 11, it can be seen that the  $\text{Cl}^-$  penetration coefficients of three kinds of AEW concrete were all lower than those of ordinary tap water concrete, of which the  $\text{Cl}^-$  penetration coefficient of B1 AEW concrete was the lowest, about  $4.10 \times 10^{-12} \text{ m}^2/\text{s}$  and  $3.4 \times 10^{-12} \text{ m}^2/\text{s}$  at

28 d and 91 d, respectively. Compared with A1 ordinary tap water concrete, the  $Cl^-$  penetration coefficients of B1, B2 and B3 AEW concrete reduced 10.5%, 7.8% and 5.3% at 91 d, respectively. The improvement effect of AEW on chloride ion penetration resistance of concrete was relatively obvious, the AEW concrete has a better anti-chloride ion permeability.

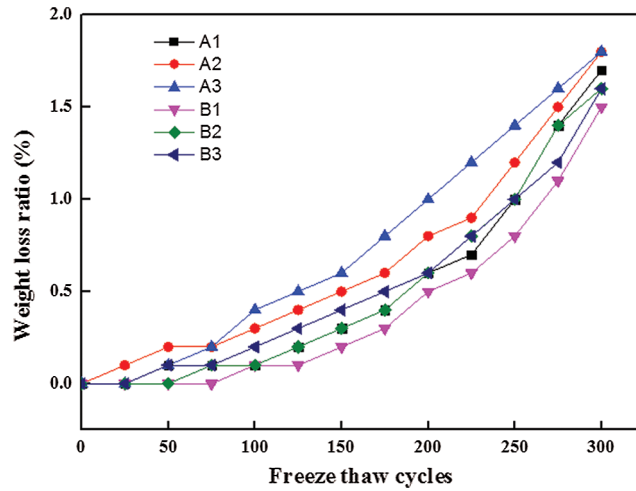


Figure 9: Weight loss ratio of concrete



Figure 10: Chloride permeability device

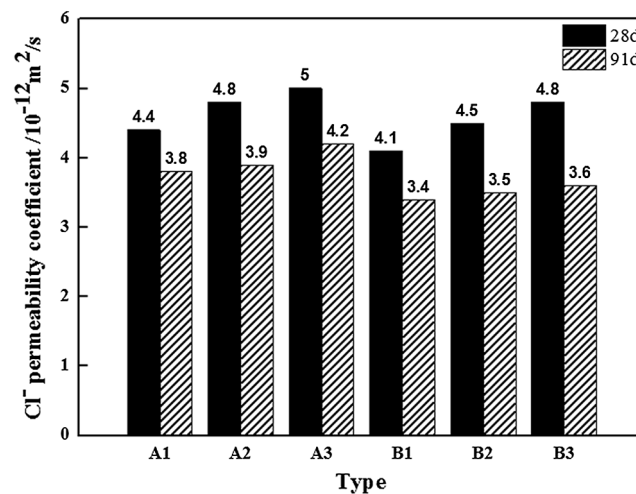
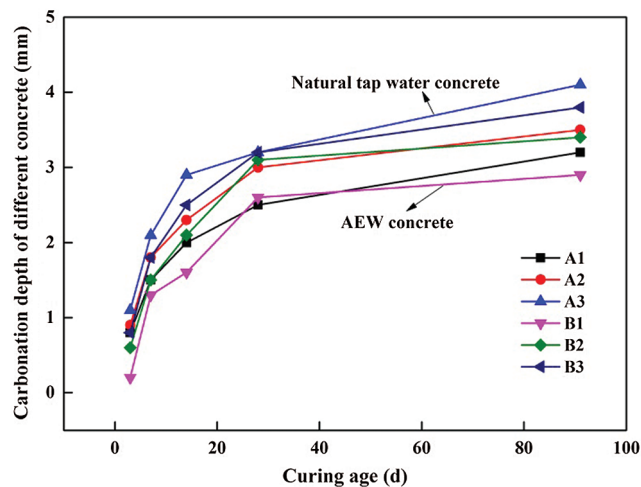


Figure 11: Chloride permeability coefficient of concrete

This is might be because that introducing the electrolyzed water in concrete can promote the cement hydration of concrete and produce the more hydration products to improve the internal pore structure and compactness of concrete, the  $\text{Cl}^-$  penetrability resistance can be improved to a certain extent. Mandal et al. [39] also reported that the durability of the concrete made with electrolyzed water is better due to lower ingress of  $\text{Cl}^-$  ions through the denser microstructure and thicker passive layer. It will be further researched by combining mercury injection and pore distribution test.

### 3.5 Carbonation Depth of Different Series of Concrete

The carbonation depths of different series of concrete are shown in Fig. 12. It can be seen that the carbonation performance of concrete can be improved by AEW. At the early age of hydration, the carbonation depths of concrete with AEW series were significantly lower than those of concrete with ordinary tap water series at same proportioning. Compared with A1 ordinary tap water concrete, the carbonation depths of B1, B2 and B3 AEW concrete at 3 d were reduced, which were 0.2, 0.6 and 0.8 mm, respectively. In contrast, at the late age of hydration, the difference in carbonation depth between the two series of concrete decreased. The carbonation depths of A1, A2 and A3 concrete at 91 d were 3.2, 3.5 and 4.1 mm, the carbonation depths of B1, B2 and B3 AEW concrete were 2.8, 3.3 and 3.8 mm.



**Figure 12:** Carbonation depth of different series of concrete

Moreover, with the increase of mineral admixture content, the carbonation depths of two series of concrete both gradually increased, this is probably related to the pore distribution and pore structure of concrete, which can be observed by the SEM micromorphology of concrete cured for 28 d in Fig. 13. From Fig. 13, it can be seen that the pore structure distribution of AEW concrete at each mix proportion was more developed and more average, the porosity of AEW concrete decreased compare with that in natural tap water concrete, this indicated that AEW can promote the hydration reaction to produce more hydration products and make the internal pore structure more dense. Chakraborty et al. [40]. believed that the enhanced durability of electrolyzed water concrete is attributed to the lower ingress of deleterious agents through the less porous and compact microstructure of the hardened composites, which is also consistent with the above result. With the increase of mineral admixture content, the porosity of two series of concrete both gradually increased, which provided a channel for the invasion of carbon dioxide in concrete, resulting in the increase of carbonization depth.

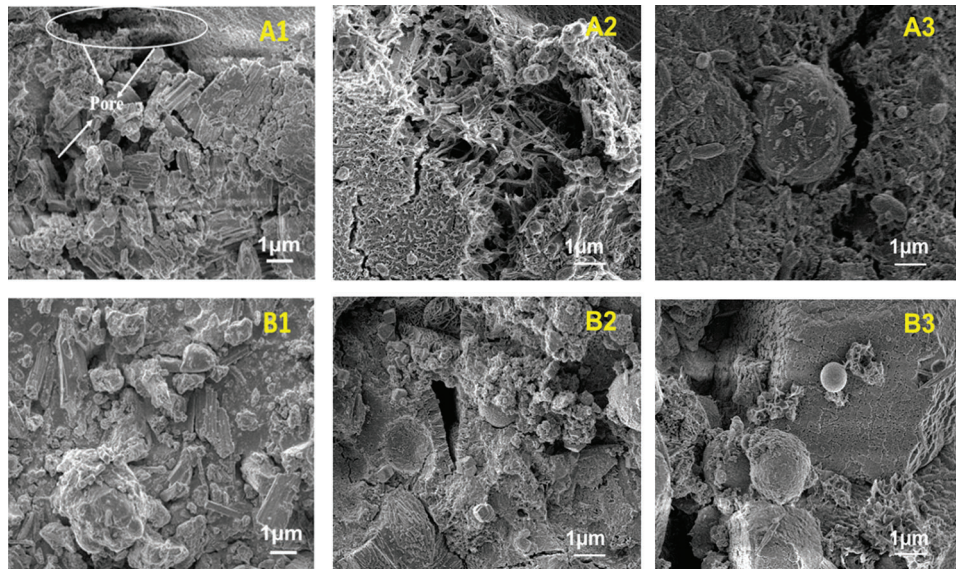


**Figure 13:** Pore structure distribution of different series of concrete by SEM micromorphology (10000 times)

### 3.6 X-ray Diffraction Analysis of Different Series of Concrete

To determine the mineral composition of concrete and assess the hydration process more accurately, an X-ray diffraction (XRD) analysis of different cement paste specimens for concrete was conducted in this study. Based on the above results of compressive strength and durability, AEW can obviously improve the early property of concrete, so the 7 d XRD testing for different cement paste specimens was conducted, the XRD patterns are shown in Fig. 14. It can be seen that three kinds of AEW concretes have obvious diffraction peaks of Afm and ettringite, the diffraction peaks of Afm and ettringite in natural water concrete were very weak. Meanwhile, the  $\text{Ca}(\text{OH})_2$  diffraction peaks of AEW concretes are enhanced obviously than those of natural water concrete, and the XRD diffraction intensity of hydrated cementitious products such as  $\text{C}_3\text{S}$  and C-A-S-H gels are obviously increased. The diffraction intensity  $\text{CaCO}_3$  (calcite) in AEW concrete was strong, which can shorten the induction period of  $\text{C}_3\text{S}$  and partially participate in the hydration. This result is essentially in agreement with the previous results that AEW may lead to a comparatively more  $\text{Ca}(\text{OH})_2$  and C-S-H hydrated products than natural water cement paste [27]. Moreover, the calcium potassium gypsum  $\text{K}_2\text{Ca}_5(\text{SO}_4)_6\cdot\text{H}_2\text{O}$  and potassium feldspar  $\text{K}_2\text{O}\cdot\text{Al}_2\text{O}_3\cdot\text{SiO}_2$  were also found easily in the XRD patterns of AEW concrete, indicating that calcium hydroxide in alkaline electrolyzed water react further with hydration products of cementitious materials, which may be beneficial to the growth of early strength of concrete. In addition, the diffraction peak intensity of hydrated products of natural tap water and AEW concrete both gradually decreased with the increase of mineral admixture content.

### 3.7 SEM Micromorphology Analysis of Different Series of Concrete

The SEM micromorphology of different series of concrete at 7 d is observed in Fig. 15. It can be seen that the microstructure of A1 concrete without mineral admixtures basically presented to be flaky and tabular, but the micromorphology of B1 AEW concrete was obvious cluster and granulation instead. This may be related to the charge adsorption of AEW on the cement surface, the electron layer adsorbed on the surface of cement particles can make the cement particles evenly disperse due to electrostatic repulsion [41]. Moreover, based on the results of XRD analysis, the alkaline electrolyzed water can promote the cement hydration and stimulate the activity of mineral admixture, probably to produce more C-A-S-H, C-S-H

gels,  $\text{Ca}(\text{OH})_2$  and other hydration products, the  $\text{Ca}(\text{OH})_2$  and AFt phases were more easily observed in the micromorphology of AEW cement pastes. The flocculent C-S-H gel intercalated with the needle AFt phase, which made the structure of the cement paste denser and benefit the increase of strength [42]. The microstructure of B2 and B3 AEW concrete with mineral admixtures was more developed and more average than A2 and A3 concrete. The result clearly justifies the appearance of the microstructural compactness of AEW cement paste.

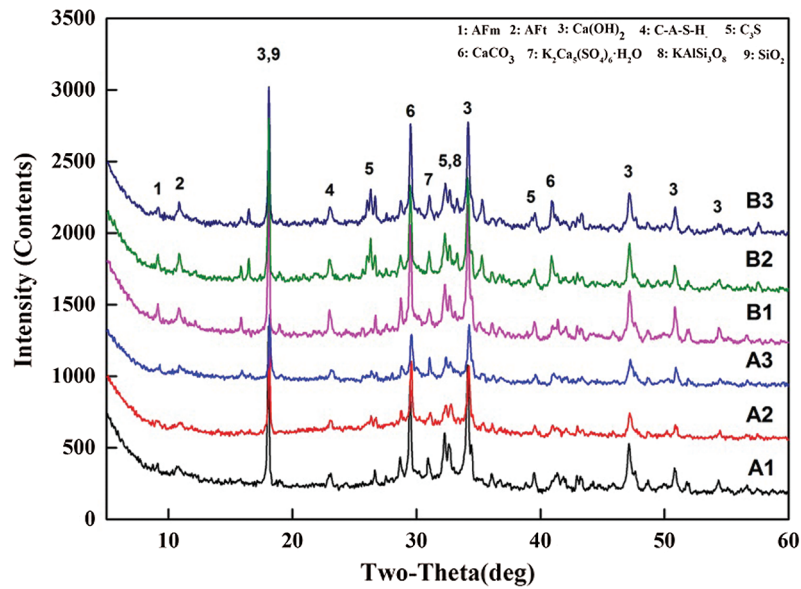


**Figure 14:** 7 d X-ray diffraction patterns of different cement paste specimens

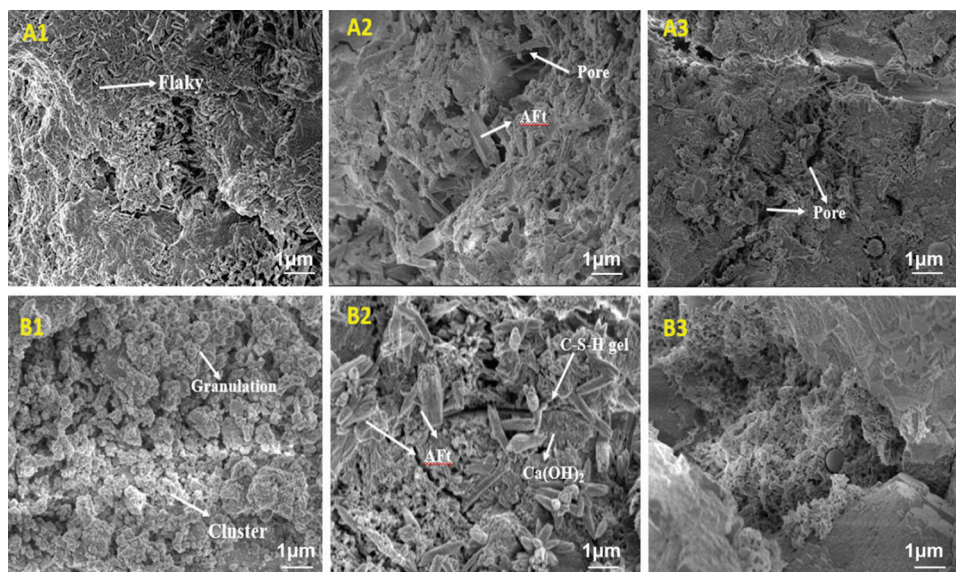


**Figure 15:** SEM images of different series of concrete (10000 times)

#### 4 Conclusions

Through a comprehensive analysis, the following conclusions can be drawn in this study:

- (1) Alkaline electrolyzed water (AEW) can accelerate hydration process of cement in paste, the cement particles are absorbed and dispersed to release more free water, leading to a workability improvement of AEW concrete than that of natural tap water concrete.
- (2) AEW in concrete can accelerate cement hydration and activate the pozzolanic effect of mineral admixtures, leading to an increase of compressive strength at early age. Compared with natural tap water cement concrete, when the replacement ratio of double-doped mineral admixture to cement are 0%, 40% and 50%, the strength of alkaline electrolyzed water concrete increased by 13.6% , 7.3% and 2.6% at 3 d, only 4.2% , 2.5% and 1.1% at 28 d.
- (3) Introducing the AEW can also improve the internal pore structure and compactness of concrete, the anti-chloride permeability, frost resistance, carbonization resistance and durability of alkaline electrolyzed water concrete with high volume mineral admixture are all lower than those of natural tap water cement concrete.
- (4) The XRD and SEM results indicate that AEW can promote the hydration reaction of cement to represent comparatively more hydrated products such as C-S-H gels,  $\text{Ca}(\text{OH})_2$  and ettringite. At the same time, the calcium potassium gypsum  $\text{K}_2\text{Ca}_5(\text{SO}_4)_6\cdot\text{H}_2\text{O}$  and potassium feldspar  $\text{K}_2\text{O}\cdot\text{Al}_2\text{O}_3\cdot\text{SiO}_2$  are also observed easily at the early age, which can benefit the improvement of strength and durability.
- (5) The fundamental mechanism of AEW to activate the pozzonlanic effect of mineral admixtures still needs further study. From the economic and environmental benefit, the AEW probably could realize the effective utilization of about 50% mineral admixture amount of concrete without strength loss, leading to reduce the cost for cement production and associated  $\text{CO}_2$  emission, which has broad application prospect.

**Acknowledgement:** This study was mainly supported by the National Natural Science Foundation of China, Natural Science Foundation of Shandong Province, Qingdao Agricultural University and Qingdao Qingjian New Material Group Co., Ltd., Qingdao, China

**Funding Statement:** This research was funded by National Natural Science Foundation of China (Grant Nos. 51808310, 51878366), Natural Science Foundation of Shandong Province (Grant Nos. ZR2019PEE007, ZR2020ME036), High-level Scientific Research Foundation for the introduction of talent of Qingdao Agricultural University (Grant No. 1118034).

**Conflicts of Interest:** The authors declare that they have no conflicts of interest to report regarding the present study.

#### References

1. Zhang, S. Y., Yang, L., Ren, F. Y. (2020). Rheological and mechanical properties of cemented foam backfill: Effect of mineral admixture type and dosage. *Cement and Concrete Composites*, 112(1–3), 103689. DOI 10.1016/j.cemconcomp.2020.103689.
2. Sahoo, S., Mahapatra, T. R., Priyadarshini, N., Mahapatra, S. (2020). Influence of water binder ratio on strength and acid resistance of concrete made up of mineral admixture as supplementary cementitious material. *Materials Today*, 26(2), 796–803.
3. Zhuang, S. Y., Wang, Q., Zhou, Y. Q. (2019). Research on the resistance to saline soil erosion of high-volume mineral admixture steam-cured concrete. *Construction and Building Materials*, 202(2), 1–10. DOI 10.1016/j.conbuildmat.2019.02.122.
4. Liu, B. J., Luo, G., Xie, Y. J. (2018). Effect of curing conditions on the permeability of concrete with high volume mineral admixtures. *Construction and Building Materials*, 167(2), 359–371. DOI 10.1016/j.conbuildmat.2018.01.190.

5. Ma, H. Y., Yu, H. F., Sun, W. (2013). Freezing-thawing durability and its improvement of high strength shrinkage compensation concrete with high volume mineral admixtures. *Construction and Building Materials*, 39(5), 124–128. DOI 10.1016/j.conbuildmat.2012.05.025.
6. Sun, J. W., Zhang, Z. Q., Hou, G. H. (2020). Utilization of fly ash microsphere powder as a mineral admixture of cement: Effects on early hydration and microstructure at different curing temperatures. *Powder Technology*, 375, 262–270. DOI 10.1016/j.powtec.2020.07.084.
7. Jiang, H. Q., Yi, H. S., Yilmaz, E., Liu, S. W. (2020). Ultrasonic evaluation of strength properties of cemented paste backfill: Effects of mineral admixture and curing temperature. *Ultrasonics*, 100(2), 105983. DOI 10.1016/j.ultras.2019.105983.
8. Demirboğa, R., Türkmen, İ., Karakoç, M. B. (2004). Relationship between ultrasonic velocity and compressive strength for high-volume mineral-admixed concrete. *Cement and Concrete Research*, 34(12), 2329–2336. DOI 10.1016/j.cemconres.2004.04.017.
9. Rashad, A. M. (2015). A brief on high-volume Class F fly ash as cement replacement—A guide for civil engineer. *International Journal of Sustainable Built Environment*, 12(4), 278–306. DOI 10.1016/j.ijse.2015.10.002.
10. Aggarwal, V., Gupta, S. M., Sachdeva, S. N. (2010). Concrete durability through high volume fly ash concrete (HVFC)—A literature review. *International Journal of Engineering, Science, and Technology*, 2(9), 4473–4477.
11. Gesoğlu, M. (2009). Properties of self-compacting concretes made with binary, ternary, and quaternary cementitious blends of fly ash, blast furnace slag, and silica fume. *Construction and Building Materials*, 23(5), 1847–1854. DOI 10.1016/j.conbuildmat.2008.09.015.
12. Boukendakji, O., Kadri, E. H., Kenai, S. (2012). Effects of granulated blast furnace slag and superplasticizer type on the fresh properties and compressive strength of self-compacting concrete. *Cement and Concrete Composites*, 24(4), 583–590. DOI 10.1016/j.cemconcomp.2011.08.013.
13. Bahador, S. D., Tze, Y. D., Susanto, T. (2014). Durability properties and microstructure of ground granulated blast furnace slag cement concrete. *International Journal of Concrete Structures and Materials*, 2, 157–164.
14. Amarnath, Y., Babu, K. G. (2011). Transport properties of high volume fly ash roller compacted concrete. *Cement and Concrete Composites*, 33(10), 1057–1062. DOI 10.1016/j.cemconcomp.2011.07.010.
15. Guo, Y. G., Cheng, L., Gao, Z. M., Guo, S. Y. (2013). Effects of different mineral admixtures on carbonation resistance of lightweight aggregate concrete. *Construction and Building Materials*, 43, 506–510. DOI 10.1016/j.conbuildmat.2013.02.038.
16. Faiz, U. A., Shaikh, S., Supit, W. M. (2015). Compressive strength and durability properties of high volume fly ash (HVFA) concretes containing ultrafine fly ash (UFFA). *Construction and Building Materials*, 82, 571–583.
17. Oderji, S. Y., Chen, B., Shakya, C., Ahmad, M. R. (2019). Influence of superplasticizers and retarders on the workability and strength of one-part alkali-activated fly ash/slag binders cured at room temperature. *Construction and Building Materials*, 229, 116891. DOI 10.1016/j.conbuildmat.2019.116891.
18. Nagan, S., Karthiyaini, S. (2014). A study on load carrying capacity of fly ash based polymer concrete columns strengthened using double layer GFRP wrapping. *Advances in Materials Science and Engineering*, 2014(2), 1–6. DOI 10.1155/2014/312139.
19. Wang, X. Y., Park, K. B. (2015). Analysis of compressive strength development of concrete containing high volume fly ash. *Construction and Building Materials*, 98, 810–819. DOI 10.1016/j.conbuildmat.2015.08.099.
20. Yang, J., Hu, H. C., He, X. Y., Su, Y. (2021). Effect of steam curing on compressive strength and microstructure of high volume ultrafine fly ash cement mortar. *Construction and Building Materials*, 266(5), 120894. DOI 10.1016/j.conbuildmat.2020.120894.
21. Varga, I. D., Castro, J., Bentz, D. P., Zunino, F. (2018). Evaluating the hydration of high volume fly ash mixtures using chemically inert fillers. *Construction and Building Materials*, 161, 221–228. DOI 10.1016/j.conbuildmat.2017.11.132.
22. Supardi, E., Yusuf, S., Massi, M. N. (2020). Evaluation of different type of electrolyzed water against bacterial colonization of diabetic foot ulcers: Study in vitro. *Medicina Clínica Práctica*, 3(1), 100090.
23. Lyu, F., Gao, F., Zhou, X. X., Ding, Y. (2018). Using acid and alkaline electrolyzed water to reduce deoxynivalenol and mycological contaminations in wheat grains. *Food Control*, 88(1), 98–104. DOI 10.1016/j.foodcont.2017.12.036.

24. Li, Y. F., Zeng, Q. H., Liu, G., Zhao, Y., Wang, J. J. (2021). Effects of ultrasound-assisted basic electrolyzed water (BEW) extraction on structural and functional properties of Antarctic krill (*Euphausia superba*) proteins. *Ultrasonics Sonochemistry*, 71(59), 105364. DOI 10.1016/j.ultsonch.2020.105364.
25. Sun, B. Q., Wang, L. J. (2015). Study on the properties of concrete mixed with alkaline redox potential water. *Journal of Building Materials*, 12, 112–115.
26. Kimura, K., Suzuki, Y., Fujikura, Y. (2013). Basic study on the radiation dose change of mortar samples of radioactive polluted ash and electrolyzed water. *Proceedings of Japan Concrete Institute*, 35, 1489–1494.
27. Romio, M., Sumit, C., Prasanta, C., Subrata, C. (2019). Development of the electrolyzed water based set accelerated greener cement paste. *Materials Letters*, 243(7837), 46–49. DOI 10.1016/j.matlet.2019.02.017.
28. Sumit, C., Romio, M., Saswata, C., Subrata, C. (2019). Investigation on the effectiveness of electrolyzed water in controlling the early age properties of cement mortar. *Construction and Building Materials*, 211(7837), 1–11. DOI 10.1016/j.conbuildmat.2019.03.237.
29. Wang, L., Kimitaka, U., Hisashi, M., Minoru, U. (2017). The experimental study on the strength improvement of concrete introducing the different electrolyzed waters. *Journal of Modern Environmental Science and Engineering (MESE)*, 3(2), 82–89. DOI 10.15341/mese(2333-2581)/02.03.2017/002.
30. Yu, R. F., Chen, H. W., Cheng, W. P., Shen, Y. C. (2009). Application of pH-ORP titration to dynamically control the chlorination and dechlorination for wastewater reclamation. *Desalination*, 244(1–3), 164–176. DOI 10.1016/j.desal.2008.05.021.
31. Zhao, K. Y., Qiao, Y., Zhang, P., Bao, J. W., Tian, Y. P. (2020). Experimental and numerical study on chloride transport in cement mortar during drying process. *Construction and Building Materials*, 258, 119655. DOI 10.1016/j.conbuildmat.2020.119655.
32. Zhang, P., Wittmann, F. H., Vogel, M., Müller, H. S., Zhao, T. J. (2017). Influence of freeze-thaw cycles on capillary absorption and chloride penetration into concrete. *Cement and Concrete Research*, 100(2), 60–67. DOI 10.1016/j.cemconres.2017.05.018.
33. Chakraborty, S., Jo, B. W., Sikandar, M. A. (2016). Hydration mechanism of the hydrogen rich water based cement paste. *Journal of Physical Chemistry C*, 120(15), 8198–8209. DOI 10.1021/acs.jpcc.6b01444.
34. Wang, L., Quan, H. Z. (2020). Effects of single and compound electrolyte electrolyzed cathode waters on mechanical property and hydration reaction of concrete. *Science of Advanced Materials*, 12(3), 366–375. DOI 10.1166/sam.2020.3550.
35. Behnam, E. J., Mohammad, R. (2020). Effect of magnetized water characteristics on fresh and hardened properties of self-compacting concrete. *Construction and Building Materials*, 242(7), 118196. DOI 10.1016/j.conbuildmat.2020.118196.
36. Prabakaran, E., Vijayakumar, A., Rooby, J. (2020). A comparative study of polypropylene fiber reinforced concrete for various mix grades with magnetized water. *Materials Today: Proceedings*.
37. Ghorbani, S., Sharifi, S., Rokhsarpour, H., Shoja, S., Gholizadeh, M. et al. (2020). Effect of magnetized mixing water on the fresh and hardened state properties of steel fibre reinforced self-compacting concrete. *Construction and Building Materials*, 248(12), 118660. DOI 10.1016/j.conbuildmat.2020.118660.
38. Wang, L., Kimitaka, U., Morozumi, H., Uemura, M. (2016). The effect of different electrolyzed water on properties and hydration reaction of mortar. *Proceedings of Japan Concrete Institute*, 38(1), 237–242.
39. Mandal, R., Chattopadhyay, S., Chakraborty, S., Chakraborty, P., Chakraborty, S. (2019). Development of electrolyzed water based concrete: A new approach for early strength gain. *UKIERI Concrete Congress*. <https://ukiericoncretecongress.com/Home/files/Proceedings/pdf/UCC-2019-193.pdf>.
40. Chakraborty, S., Mandal, R., Chakraborty, S., Guadagnini, M., Pilakoutas, K. (2021). Chemical attack and corrosion resistance of concrete prepared with electrolyzed water. *Journal of Materials Research and Technology*, 11(8), 1193–1205. DOI 10.1016/j.jmrt.2021.01.101.
41. Lyu, K., She, W., Miao, C. W., Chang, H. L., Gu, Y. (2019). Quantitative characterization of pore morphology in hardened cement paste via SEM-BSE image analysis. *Construction and Building Materials*, 202(4), 589–602. DOI 10.1016/j.conbuildmat.2019.01.055.
42. Luís, P. E. (2011). On the hydration of water-entrained cement-silica systems: Combined SEM, XRD and thermal analysis in cement pastes. *Thermochimica Acta*, 518(1–2), 27–35. DOI 10.1016/j.tca.2011.02.003.